Published in final edited form as:

Acta Biomater. 2017 August ; 58: 1–11. doi:10.1016/j.actbio.2017.06.025.

Enhanced Nutrient Transport Improves the Depth-Dependent Properties of Tri-Layered Engineered Cartilage Constructs with Zonal Co-Culture of Chondrocytes and MSCs

Minwook Kim[1,2,3], **Megan J. Farrell**[1,2,3], **David R. Steinberg**[1,3], **Jason A. Burdick**[2,3], and **Robert L. Mauck**[*,1,2,3]

[1]McKay Orthopaedic Research Laboratory, Department of Orthopaedic Surgery, Perelman School of Medicine, University of Pennsylvania, Philadelphia, PA 19104, U.S.A

[2]Department of Bioengineering, University of Pennsylvania, Philadelphia, PA 19104, U.S.A

[3]Translational Musculoskeletal Research Center (TMRC), Corporal Michael J. Crescenz Veterans Affairs Medical Center, Philadelphia, PA 19104, U.S.A

Abstract

Biomimetic design in cartilage tissue engineering is a challenge given the complexity of the native tissue. While numerous studies have generated constructs with near-native bulk properties, recapitulating the depth-dependent features of native tissue remains a challenge. Furthermore, limitations in nutrient transport and matrix accumulation in engineered constructs hinders maturation within the central core of large constructs. To overcome these limitations, we fabricated tri-layered constructs that recapitulate the depth-dependent cellular organization and functional properties of native tissue using zonally derived chondrocytes co-cultured with MSCs. We also introduced porous hollow fibers (HFs) and HFs/cotton threads to enhance nutrient transport. Our results showed that tri-layered constructs with depth-dependent organization and properties could be fabricated. The addition of HFs or HFs/threads improved matrix accumulation in the central core region. With HF/threads, the local modulus in the deep region of tri-layered constructs nearly matched that of native tissue, though the properties in the central regions remained lower. These constructs reproduced the zonal organization and depth-dependent properties of native tissue, and demonstrate that a layer-by-layer fabrication scheme holds promise for the biomimetic repair of focal cartilage defects.

Graphical abstract

[*]**Address for Correspondence**: Robert L. Mauck, Ph.D., Mary Black Ralston Professor of Orthopaedic Surgery, Professor of Bioengineering, McKay Orthopaedic Research Laboratory, Department of Orthopaedic Surgery, Perelman School of Medicine, University of Pennsylvania, 36th Street and Hamilton Walk, Philadelphia, PA 19104, Phone: (215) 898-3294, Fax: (215) 573-2133, lemauck@mail.med.upenn.edu.

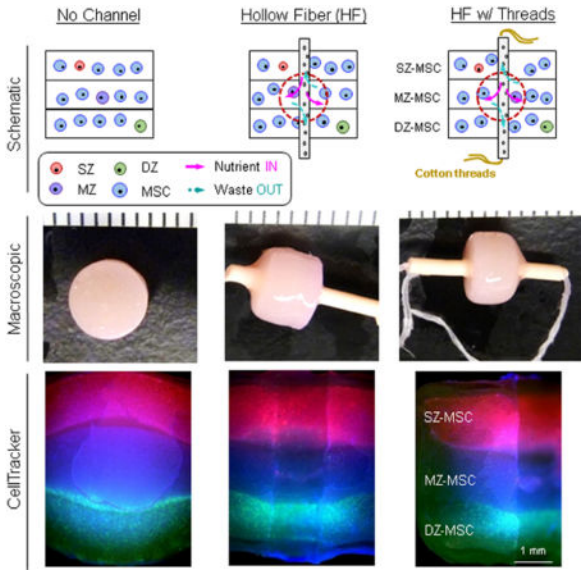

Keywords

Cartilage tissue engineering; Co-culture; Mesenchymal stem cells; Zonal Chondrocytes; Depth-dependent properties; Nutrient transport; Hyaluronic acid

1. Introduction

Articular cartilage provides a nearly frictionless load-bearing surface in diarthrodial joints. This functionality is attributed to extracellular matrix (ECM) molecules (e.g., collagens, proteoglycans (PG), lubricin [1] and elastin [2, 3]) that are secreted by chondrocytes (CH) residing within the tissue. These cells have a distinct size, morphology, orientation, and matrix forming capacity, based on their zone of origin (e.g., superficial (SZ), middle (MZ), and deep zone (DZ)) [4, 5]. The tissue itself also shows marked differences in composition and mechanics as a function of depth, where it is proteoglycan-rich and stiffest in compression in the deep zone, and collagen-rich and weakest in compression (and strongest in tension) in the superficial zone. Given the complexity of native tissue, recapitulating the morphological and functional properties of articular cartilage has remained a challenge in cartilage tissue engineering [5, 6]. Indeed, most early studies in the field focused on optimizing bulk properties of cell-laden constructs using a mixed pool of cells, ignoring zonal features. While these constructs achieved overall construct properties approaching native levels, they did not match native tissue depth-dependence. More recently, several groups have taken advantage of persistence of zonal characteristics of CHs isolated from different regions of the tissue. These studies have shown that CHs from different depths retain their zonal characteristics through expansion and in 3D culture systems. For example, CHs isolated from deep zone cartilage produced more PG than those from the superficial zone [7–11]. Interestingly, when these zonal CHs were separately seeded into layered hydrogel constructs, zonal CHs established engineered constructs with some degree of depth dependence [7, 8, 11–15].

While CHs have been broadly used as a primary cell source in cartilage tissue engineering, their scarcity is a major clinical limitation. For that reason, mesenchymal stem cells (MSCs) have been introduced as an alternative cell source for cartilage therapeutics. Unlike CHs, MSCs can be isolated from autologous sources and readily expanded while maintaining their differentiation potential. When cultured in the presence of defined factors (i.e., transforming growth factor beta 3; TGF-β3) [16, 17], these cells can undergo chondrogenesis and produce cartilage-like ECM [18]. It has also been shown that, when MSCs are cultured in 3D with CHs in a 'co-culture' scenario, the two cell types interact and improve matrix formation [19]. This suggests that by adapting a layer-by-layer fabrication scheme, and utilizing MSCs co-cultured with zonal CHs, one might recapitulate the zonal organization and depth-dependent properties of native tissue while decreasing the number of CHs required for tissue formation.

While the choice of cell type and 3D fabrication methods has expanded, a persistent challenge across cartilage tissue engineering is the effective transport of nutrients into (and metabolic waste out of) constructs. This is particularly true for larger constructs, where the core regions show limitations in matrix formation [20–22]. Several studies have reported that a greater amount of matrix with higher stiffness is produced in the peripheral regions of constructs compared the central core regions, where there is a lower abundance of matrix and its properties are less robust [22–25]. In engineered cartilage established by MSCs, whose metabolic state is more tenuous than CHs, this nutrient deprivation often results in cell death in the central core with extended culture durations. This suggests that insufficient soluble factor transport compromises and/or limits cell function in engineered constructs, ultimately resulting in inhomogeneous matrix accumulation [20, 24]. This issue is critical when considering scaling up to repair thicker cartilage regions (e.g., the femoral condyle) [23, 26] or larger defect areas (e.g., partial or total joint resurfacing) [27, 28].

To improve nutrient transport and functional properties, a number of possible strategies have been explored. For example, some have used dynamic loading-induced convective transport to encourage fluid movement [29, 30]. Others have employed encapsulated microbubbles to create additional paths for diffusion [31] or have simply reduced construct thickness to shorten the nutrient path length [24]. Perhaps most prominently, several studies have introduced macro-scaled (0.5mm or more) channels into tissue engineered constructs in order to introduce new paths for nutrient transport [23, 26, 32]. Interestingly, Cigan and co-workers recently demonstrated that the one time creation of these macro channel(s) did not improve matrix accumulation in the core, and reported that this was due to the eventual blockade of the channel by newly formed tissue after a short period of culture [23, 24, 26]. A follow up study from that same group reported that reopening the closed macro-channels midway through culture (by 're-punching' the channels) refreshed nutrient transport and improved functional properties over the long term [22]. Collectively, these data indicate that prolonged provision of ready nutrient access to the center of large constructs will be essential for functional tissue formation in large constructs.

Based on the above challenges and limitations, our first objective in this study was to fabricate a tri-layered construct that recapitulates the cellular organization and depth-dependent functional properties of native articular cartilage, using the layered co-culture of

zonal CHs and MSCs. Our second objective, acknowledging the nutrient limitations likely experienced by these larger constructs, was to enhance nutrient/waste transport to improve viability and matrix deposition by cells within the central core region. For this, we introduced a porous hollow fiber (HF) [33] as a conduit to enable persistent diffusion of soluble factors into the central core [34–36]. To avoid blockade of these channels, we also inserted cotton threads through the inner core of the HF to continuously wick media to the center of construct while maintaining an open channel for nutrient exchange. Our findings demonstrate the production of a tri-layered cell-based construct with depth-dependent morphology and functional properties, furthering our goal of generating biomimetic engineered cartilage to improve cartilage repair and long-term stability post-implantation.

2. Materials and Methods

2.1. Preparation of zonal chondrocytes (CHs) and mesenchymal stem cells (MSCs)

Chondrocytes (CHs) and MSCs were isolated from juvenile bovine stifle joints (3 months old, Research 87, Bolyston, MA). CHs and MSCs obtained from multiple donors were pooled for these studies [37]. Full-thickness cartilage plugs were excised from the femoral condyle and divided into three layers (Fig 1A). The top-most 100μm thick layer at the articular surface was carefully divided and taken as the superficial zone. The block from the bony surface to just above the tidemark was removed and discarded. The resulting “top” half was considered as middle zone and the “bottom” half as deep zone cartilage [8, 12]. Zonal CHs were isolated by collagenase digestion from these separated zonal cartilage tissues, and MSCs were isolated from bone marrow as in our previous studies [38, 39]. These isolated zonal CHs and MSCs were separately maintained and expanded in basal media consisting of high glucose Dulbecco’s Modified Eagle Medium (DMEM; ThermoFisher, Grand Island, NY) supplemented with 10% fetal bovine serum (FBS; ThermoFisher, Grand Island, NY) and 1% penicillin/streptomycin/fungizone (PSF; ThermoFisher, Grand Island, NY). At passage 3, zonal CHs and MSCs were trypsinized and washed with phosphate buffered saline (PBS) (ThermoFisher, Grand Island, NY). To trace the distribution of each cell subpopulation, cells were labeled with CellTracker (Molecular Probes, Eugene, OR) prior to encapsulation (SZ = red, MZ = purple, DZ = green, MSC = blue). Cell viability was examined with Calcein-AM using the LIVE/DEAD Assay Kit (Molecular Probes, Eugene, OR) after 8 weeks of culture.

2.2. MeHA synthesis and cell encapsulation

Details on the synthesis of photocrosslinkabe hyaluronic acid (HA) macromer have previously described as in Burdick et al., [40]. Briefly, 1 % w/v sodium hyaluronate (65 kDa HA; Lifecore Biomedical, Chaska, MN) solution was reacted with methacrylic anhydride (Sigma, St. Louis, MO) on ice at pH 8.0 for 24 hours followed by dialysis to remove unreacted byproducts for 5 days. Following dialysis, the methacrylated HA (MeHA) solution was lyophilized and stored at −20°C. The lyophilized MeHA was dissolved at 1% w/v in PBS with 0.05% w/vol photoinitiator (Irgacure I2959, CibaGeigy, Tarrytown, NY). The CellTracker-labeled zonal CHs and MSCs were encapsulated in 1% MeHA at a concentration of 60 million cells/mL and exposed to UV using a 365 nm BlakRay UV lamp

(#UVL56, San Gabriel, CA). The range of the UV was 320–400 nm with a transmission maximum of 70% at 365 nm.

2.3. Fabrication of a tri-layered construct with zonal co-culture of CHs and MSCs

Previous studies have shown that freshly isolated zonal chondrocytes (CHs) retained their zonal characteristics in 3D culture [8, 11]. Based on these findings, we fabricated a tri-layered construct [7] by partially polymerizing a zonal CH and MSC mixture in sequential layers of HA hydrogel (SZ-MSC, MZ-MSC and DZ-MSC, respectively) (Fig 1B). MSC alone, or co-cultured cell populations, were encapsulated in 1% w/v MeHA at 60×10^6 cell/mL, with a ratio of 1: 4 (CH: MSC) for the co-cultured group. Tri-layered constructs were created by exposing the first layer (20 μL; SZ-MSC mixture = 1:4) of MeHA solution to UV light for 2 minutes, followed by polymerization of the second layer (20 μL; MZ-MSC) for 2 minutes, and finally adding the third layer (20 μL; DZ-MSC) with completion of polymerization for another 6 minutes. (Ø4.8 mm × 3.5 mm). Polymerization took place within a 1 mL syringe, and the top surface of each layer was exposed by UV light during the polymerization. All other groups (MSC alone, SZ-MSC, MZ-MSC and DZ-MSC; 60 μL/construct) were polymerized under continuous UV light for 10 minutes. Constructs were then transferred directly to a 12 well plate and cultured in chemically defined media (CM) (2 mL/construct) containing high glucose DMEM supplemented with 1% PSF, 0.1 μM dexamethasone, 50 μg/mL ascorbate 2-phosphate, 40 μg/mL L-proline, 100 μg/mL sodium pyruvate, 6.25 μg/mL insulin, 6.25 μg/mL transferrin, 6.25 ng/mL selenious acid, 1.25 mg/mL bovine serum albumin (BSA), and 5.35 μg/mL linoleic acid [16, 41] with TGF-β3 (CM_+; 10 ng/mL, R&D Systems, Minneapolis, MN). Constructs were turned regularly to improve growth through the depth and media was replaced thrice weekly for the duration of study.

2.4. Enhanced nutrient transport via the introduction of a porous hollow fiber (HF)

During the in vitro culture, cell-laden cylindrical constructs were cultured in 12-well plates. When the constructs were placed and not moved, the bottom surface of the construct had less access to nutrients in the media compared other regions of the constructs (e.g., the top and circumferential surfaces) under static culture conditions (e.g., no mechanical agitation). To improve the nutrient transport, the constructs were regularly flipped during the culture period to maximize nutrient access. However, even with flipping, early studies resulted in little matrix accumulation in the core region of the construct compared to peripheral region. To address this limitation, we introduced a porous hollow fiber (HF) (FiberCell Systems Inc., Frederick, MD) through the core along the axial direction of the construct after 3 days of culture. The HF (polysulfone, OD = 1.3 mm, ID = 0.7mm, wall thickness = 300μm, pore size = 0.1μm) was activated by soaking in 70% ethanol for 24 hours to open the pores for nutrient and waste transport. The HF serves as a conduit, and was maintained in a hydrated state to keep the pores open after activation. Next, the HF was washed with sterile distilled water and was pre-cultured in CM_+ at 37°C/5% CO_2 for 24 hours. To ensure media delivery and to prevent clogging of the channel with air bubbles, fresh media were injected through the inner core of the HF at each media change. In addition, cotton threads pulled from a sterile gauze pad were inserted through the inner annulus of the HF to help wick media and to maintain an open channel pathway absent of tissue or air bubble obstruction.

2.5. Analysis of bulk mechanical properties

To determine bulk mechanical properties, constructs were tested in unconfined compression using a custom-built device [42]. Constructs were equilibrated under a static load of 2 grams for 5 minutes. Following this creep test, samples were subjected to 10% strain at 0.05%/s, calculated from the post creep thickness of the construct. This deformation phase was followed by a relaxation for 1000 seconds to allow the construct to reach equilibrium. After stress-relaxation, dynamic testing was carried out by applying a superimposed 1% sinusoidal deformation at 1.0 Hz. Equilibrium and dynamic moduli were calculated from the stress–strain response during the test and the sample geometry. For the tri-layered constructs with HF and HF/threads, the surface area of the HF was subtracted from the total surface area in these calculations.

2.6. Analysis of local mechanical properties

Local mechanical properties [43] were measured using a custom-built compression device [44] coupled with an inverted microscope (Nikon Eclipse TE 2000-U, Nikon, Melville, NY). Subsequent to bulk compression testing, cylindrical constructs were cut in a half, and cell nuclei were stained with Hoechst 33342 (10 μL/mL; Molecular Probes, Eugene, OR) for 10 min. Stained constructs were placed in a PBS-filled chamber in the device, and the cross-section of the construct was oriented facing down (towards the microscope objective). Details on the measurement of local properties were previously described as in [43, 44]. Briefly, the construct was uniaxially compressed while tracking displacement of nuclei on 2X magnification images captured at equilibrium (after 7 min relaxation) for compressive steps of 4% ranging from 0% to 20% strain. The load was recorded at each step once the construct had reached equilibrium. Stained nuclei served as fiducial markers to generate ‘speckle’ that was than tracked in the image series via digital image correlation using Vic-2D (Correlated Solutions, Columbia, SC). From these displacement fields, the local Lagrangian strain (E_{xx}) was calculated, where x is the axial direction of the hemi-cylindrical construct (depth from the S-M to D-Z region). Local strains were exported to MATLAB (The Math Works Inc., Natick, MA) and the average values were computed according to depth (defined as region 1 through 10 from the top to bottom of the construct). Local modulus was calculated using these resultant strain values and equilibrium boundary stresses. The reported local modulus was limited to the inner 70% (region 2 to region 8) of the construct thickness due to edge effects of the testing modality. To validate findings of depth dependency, we first tested bi-layered constructs with prescribed depth dependent material properties formed from 1% and 5% MeHA (2:1 ratio = 40 μL: 20 μL, 20 million cells/mL in each sub-layer). These constructs were tested and analyzed as described above. Full thickness articular cartilage plugs (Ø5 mm) were collected from juvenile bovine femoral condyle. After trimming the subchondral region, the local mechanical properties were assessed (n=3) as a comparison to the engineered tissues.

2.7. Biochemical analysis

Subsequent to local mechanical testing, the construct wet weight (WW) was measured, followed by papain digestion (1 mL/construct, 0.56 U/mL in 0.1M sodium acetate, 10M cysteine hydrochloric acid, 0.05 M ethylenediaminetetraacetic acid, pH 6.0) at 60°C for 16

h. Glycosaminoglycan (GAG) content was determined using the 1, 9 dimethylmethylene blue (DMMB) dye binding assay [45] and collagen content using the orthohydroxyproline (OHP) assay, with a 1 : 7.14 (OHP : collagen) ratio, as previously described [46].

2.8. Histological analysis

Constructs were fixed in 4% paraformaldehyde (PFA) and embedded in paraffin. Sections (8 μm thick) were deparaffinized in a graded series of ethanol and stained with Alcian Blue (pH 1.0) for proteoglycans (PG) with a nuclear fast red counterstain. Immunohistochemistry was carried out to visualize type II collagen and chondroitin sulfate (CS). Samples underwent antigen retrieval using hyaluranidase (HASE) from type IV bovine testes (300μg/mL; Sigma-Aldrich, St. Louis, MO) for 1 hour and followed by Protease-K (S3020; DAKO, Glostrup, Denmark) digestion for 4 minutes at room temperature. Endogenous peroxidase activity was quenched by pretreating sections with 3% hydrogen peroxide. To block nonspecific staining, sections were incubated with 10% normal goat serum (Sigma-Aldrich, St. Louis, MO). Primary antibodies for type II collagen (II-II6B3; Developmental Studies Hybridoma Bank, Iowa City, IA), and chondroitin sulfate (C8035, Sigma-Aldrich, St. Louis, MO) were applied; antibody diluent solution (DAKO, Glostrup, Denmark) was used to dilute primary antibodies. After incubation with primary antibodies overnight at 4°C, sections were washed and treated with bioinylated goat anti-rabbit IgG secondary antibodies, followed by streptavidin horseradish peroxidase (HRP). Sections were reacted with DAB chromogen reagent for 10 ~20 min (Millipore, Billerica, MA) and imaged on a light microscope (Leica DMLP, Leica Microsystems, Germany) equipped with a color charged-coupled device (CCD) digital camera.

2.9. Statistical analysis

Statistical analysis was performed using the SYSTAT software (v10.2, SYSTAT software Inc., San Jose, CA). Significance was determined by two-way ANOVA with Tukey's post hoc test ($p < 0.05$).

3. Results

3.1. Fabrication of tri-layered constructs with zonal CHs/MSCs co-cultured sublayers

Mechanical and biochemical properties of co-cultured (SZ-MSC, MZ-MSC and DZ-MSC) constructs depended on the zonal origin of chondrocytes: the least matrix production and lowest mechanics was seen in constructs from the SZ-MSC group (316kPa, 4.2%WW for GAG and 3.3%WW for collagen), and the highest mechanics/matrix production was seen in MZ-MSC (480kPa (p=0.058), 4.8%WW GAG and 6.5%WW collagen (p=0.047)) and DZ-MSC (427kPa, 4.5%WW GAG and 7.3%WW collagen, p=0.006) groups at 16 weeks. Overall bulk properties of the tri-layered construct reached 537kPa, 4.4%WW GAG and 6.4%WW, whereas MSC-only constructs reached only 338kPa, 3.7%WW GAG and 7.6%WW collagen at 16 weeks, respectively (Table 1). MSCs and CHs remained viable over the 16 week culture period, and each cell population was well distributed within its appropriate layer (Fig 2A–C). Both tri-layered and MSC-only constructs showed dense type II collagen (COL II) and chondroitin sulfate (CS) deposition at 8 weeks (Fig 2D). While there was a robust matrix accumulation throughout the constructs, matrix accumulation was

markedly limited in the core region. When observing the cross-section of these constructs, the peripheral region was much stiffer than the core, as evidenced by the core region swelling outward when the constructs were divided in a half (Fig 2E). Alcian blue staining confirmed greater PG deposition in the peripheral region compared to the core (Fig 2F). Further, the cells in the peripheral region retained a rounded morphology reminiscent of the native tissue, whereas the cells in the core region were enlarged, with disorganized lacunae indicating a possible hypertrophic or unhealthy state.

3.2. Enhancement of nutrient transport via the inclusion of a hollow fiber (HF)

To improve nutrient/waste transport in the core regions of these constructs, we introduced a porous hollow fiber (HF) with or without the addition of a cotton thread (Fig 3). HFs in the tri-layered constructs remained open during the culture periods (Fig 4A). There was little to no interaction between the HF and the hydrogel construct, as shown by a clear interface between the two upon removal of the HF (Fig 4B). To investigate the ability of the HFs (with or without thread) to promote nutrient/waste transport, particularly in the core region, we assessed three different conditions. These included constructs with no channel, with HF alone, and with HF w/cotton thread (Fig 5). Based on visual inspection, constructs from all groups grew well and achieved similar volumes (Fig 5A). However, the core regions of the constructs with no channel showed much less matrix deposition compared to the peripheral regions. Conversely, those constructs with HF or HF w/cotton threads showed greater matrix accumulation, with the center comparable to the construct edge. The core region with HF w/ cotton thread appeared fully matured and homogenous throughout the cross-section (Fig 5B). Each layer within constructs with HF and HF w/cotton threads remained flat, while those without a channel showed swelling of the MZ-MSC layer, resulting in deformations of the adjacent SZ-MSC and DZ-MSC layers. The mixed populations of CHs and MSCs were well distributed within their appropriate layers in all groups (Fig 5C). Calcein-AM staining showed A greater number of viable cells were seen in the core region of constructs with HF and HF w/ cotton threads (Fig 5D). Furthermore, Alcian blue staining showed marked PG production in the core region for constructs with HF and HF w/cotton threads, and cells in these regions maintained a normal morphology, whereas in constructs with no channel, there was poor matrix accumulation in the core region with cells taking on an enlarged (hypertrophic) appearance (Fig 6A). Immunohistochemical staining of type II collagen showed a greater matrix deposition in the core region with HF and HF w/cotton threads (Fig 6B), and little to no type I collagen was observed through the construct. (Fig 6C).

3.3. Functional properties of tri-layered constructs

Functional properties of tri-layered construct for all groups increased with time, with levels at the end of the study comparable to native cartilage tissue (shaded area) (Fig 7A–C). Bulk mechanical properties of no channel, HF, and HF w/cotton thread groups reached 630kPa ($p=0.014$), 600kPa, and 584kPa at 16 weeks, respectively (Fig 7A). Similarly, GAG and collagen contents (GAG/collagen, in %WW) were 3.9% /4.5%, 4.0% /3.7%, and 4.4% /4.0% at 16 weeks, respectively (Fig 7B and C). While HF and HF w/thread increased matrix distribution in the core, this improved growth at the center and did not influence bulk properties. The local modulus of these tri-layered constructs exhibited depth-dependent increases from the superficial region (SZ-MSC layer; ~0.3MPa) to the deep region (DZ-

MSC layer; ~1.4–2.3MPa; †p<0.05) (Fig 7F). The properties of constructs with HF w/cotton threads (green) in the deep zone (DZ-MSC) nearly matched native levels (black/dashed line). While the overall depth dependence mirrored native tissue, the properties in the central regions were still lower than that of the native tissue in all groups (*p<0.05).

4. Discussion

In this study, we developed methods to co-culture zonal CHs with MSCs in 3D HA hydrogels, and fabricated a tri-layered construct (with mixed cell subpopulations in each layer) to mimic the zonal organization and depth-dependent properties of native cartilage. To verify the proper separation of zonal cartilage and isolation of zonal CHs, the GAG content of each layer was evaluated by DMMB assay, and the isolated zonal CHs were assessed in terms of morphology. Following isolation, zonal CHs alone or co-cultured with MSCs were encapsulated in MeHA and cultured in CM_+ for 8 weeks. Although we did not specify zonal CH markers from the isolated CHs, gross morphology of the isolated zonal CHs and zonal variations in GAG content from native cartilage as well as isolated zonal CH-laden in HA construct verified the proper isolation of zonal CHs (Supplementary 1). Constructs formed from superficial CHs and MSCs yields tissue with the lowest compressive properties and GAG content (320 kPa; 4.2% WW), while those formed from middle or deep zone CHs and MSCs had the highest bulk properties (>430 kPa; >4.5%). This indicates the passaged chondrocytes re-differentiated in the presence of TGF-β3 while retaining their zonal characteristics, even after multiple population doublings [7, 47, 48]. Importantly, the differences that emerged between cultures were apparent with CHs comprising only 20% of the starting cell population. This suggests that CH-MSC co-cultures of zonal origin might be harnessed to replicate native tissue form and function.

Building from this platform, single-layered constructs (with zonal co-culture) were combined into one tri-layered construct. Under this scenario, zonal CHs in each layer retained their distinct cellular matrix forming capacity and organization and remained viable over 16 weeks, as did the co-cultured MSCs. The fact that MSCs remained viable and produced ECM may suggest that molecular factors secreted from CHs promote their function under these challenging conditions [49]. Sustained ECM production by MSCs in this co-culture context could potentially reduce the need of CHs by up to 80%. Overall, we noted robust accumulation of type II collagen (COL II) and chondroitin sulfate (CS) throughout the cross-sectional area, though all constructs showed a core region in which little matrix was deposited. Cells in the peripheral regions maintained a small size and round shape with a distinct cell boundary and nuclei, whereas those in the core appeared much larger. While both MSC-laden and mixed cell-laden constructs were maintained under the same culture conditions, the equilibrium modulus and GAG content of tri-layered constructs were 1.7 and 1.3 times greater than that of the MSC-laden constructs, respectively. This may be due to MSCs cultured alone being more sensitive to changes in their microenvironment (e.g., glucose level or oxidative stress) [50] compared to those mixed with CHs.

Despite these positive findings with tri-layered co-cultures, the need for improved nutrient transport was evident, as demonstrated by the differing matrix production in the central and peripheral regions. This is due to the limited transport of nutrient and metabolic byproducts

secreted by the cells in the central region as new matrix was initially formed and deposited in the peripheral region. Thus, this transport challenge exists regardless of cell type, and has been reported by many others, particularly when engineering larger constructs [20, 23, 26, 32]. Early efforts to overcome this issue have centered on the application of dynamic loading, decreasing construct thickness, or creating macro-channels. While channels appear promising during short term culture, we and others have shown that macro-channels can become filled with newly formed tissue early in culture (Supplementary 2). This can be addressed to some extent by 're-punching' the closed channels [21], though this requires an additional handling step during culture. To overcome this limitation, in this study we included a porous HF or a HF strung with a cotton thread to maintain channel patency and improve nutrient/waste transport into the core of the construct. Introduction of the central HF or HF/thread preserved construct dimensions (limited swelling in each layer) and improved cell viability, particularly in the core region. Cells in the core region retained a normal morphology and produced abundant matrix, whereas cells in constructs lacking a channel were enlarged, with poor matrix production. However, while the HF and/or HF w/ thread promoted more uniform matrix accumulation and maintained cell morphology, there was no effect on bulk properties. This suggests that the bulk properties were mainly governed by properties of the periphery, which may act as a mechanical strut during bulk testing. That said, when we measured the local properties of the tri-layered constructs, we found that the deep zone of constructs with HF w/cotton thread nearly matched that of the native bovine cartilage deep zone (DZ-MSC) [8]. Indeed, the ratio of local modulus from the top to bottom layer of the tri-layered construct (DZ:MSC / SZ:MSC) with no channel, with HF, and with HF w/thread was 4, 6.5 and 6.8, respectively. In native bovine cartilage, this ratio is 7.9 (DZ/SZ). While constructs overall began to mirror the depth dependence of native tissue, the properties of the central region (MZ-MSC layer) were still lower than that of the native tissue. Insertion of the HF or HF w/thread did not improve the mechanical properties of the middle region, despite improved matrix deposition in these central regions. This again suggests that the edge of the construct develops the highest properties and dominates both bulk and local mechanical response in constructs of this size. This may in the future be addressed by adding additional nutrient channels [21] and/or extending the culture duration and system to examine larger constructs where the edges are further removed.

Biomimetic design in engineering cartilage-like constructs is of importance not only for recapitulating native structure and function but also for enhancing integrative repair by modulating zone-to-zone integration and spatially matching mechanical properties with the host tissue. By filling defects in a zonally consistent manner, one might promote better integration between the repair and host tissue under physiologic loading. That is, if the depth-dependent properties of the implant mirror the native tissue, this would harmonize deformations through the depth and diminish stress concentrations at the integrative surface. In this regard, the current design is still in need of fine tuning with respect to the thickness of each layer, based on the generally defined 10% (superficial zone), 60% (middle) and 30% (deep zone) layers of native tissue. Further studies will be required to validate this concept using native cartilage and more precisely engineered depth-dependent engineered tissue constructs. Lastly, this study utilized juvenile CHs and MSCs. However, the majority of

patients suffering from OA are elderly, and the chondrogenic capacity of MSCs attenuates with aging. In other studies, we have explored the possibility of combining CHs from juvenile sources with adult MSCs in a co-culture scenario. Our preliminary results indicate that these juvenile CHs can have a beneficial effect on adult MSCs. To translate this approach, it will be essential to validate this co-culture phenomenon using human sources. Interestingly, there is a commercially available product on the market that is comprised of living, morselized, juvenile cartilage fragments (DeNovo NT, Zimmer). Given this, it is possible that the sourcing of the CH subpopulation could be allogenic, and could be combined with autologous MSCs taken from the iliac crest (or some other location not likely to cause iatrogenic issues).

5. Conclusions

Taken together, our results demonstrate that a layer-by-layer fabrication scheme, including co-cultures of zone-specific articular CHs and MSCs, can reproduce the depth-dependent characteristics and mechanical properties of native cartilage while minimizing the need for large numbers of chondrocytes. Such a tri-layered construct may provide critical advantages for focal cartilage repair. These constructs hold promise for restoring native tissue structure and function, and may be beneficial in terms of zone-to-zone integration with adjacent host tissue and providing more appropriate strain transfer after implantation. Future work will investigate how individual cells within each layer communicate with one another and with adjacent layers, and will scale this technology to produce constructs of anatomic relevance for cartilage repair applications [27, 28, 51].

Supplementary Material

Refer to Web version on PubMed Central for supplementary material.

Acknowledgments

This work was supported by the National Institutes of Health (R01 EB008722), the Department of Veterans' Affairs (I01 RX000700), and the Force and Motion Foundation (AMTI).

References

1. Rhee DK, Marcelino J, Baker M, Gong Y, Smits P, Lefebvre V, Jay GD, Stewart M, Wang H, Warman ML, Carpten JD. The secreted glycoprotein lubricin protects cartilage surfaces and inhibits synovial cell overgrowth. J Clin Invest. 2005; 115(3):622–31. [PubMed: 15719068]
2. He B, Wu JP, Chen HH, Kirk TB, Xu J. Elastin fibers display a versatile microfibril network in articular cartilage depending on the mechanical microenvironments. J Orthop Res. 2013; 31(9): 1345–53. [PubMed: 23649803]
3. Mansfield J, Yu J, Attenburrow D, Moger J, Tirlapur U, Urban J, Cui Z, Winlove P. The elastin network: its relationship with collagen and cells in articular cartilage as visualized by multiphoton microscopy. J Anat. 2009; 215(6):682–91. [PubMed: 19796069]
4. Mow VC, Wang CC, Hung CT. The extracellular matrix, interstitial fluid and ions as a mechanical signal transducer in articular cartilage. Osteoarthritis Cartilage. 1999; 7(1):41–58. [PubMed: 10367014]
5. Poole AR, Kojima T, Yasuda T, Mwale F, Kobayashi M, Laverty S. Composition and structure of articular cartilage: a template for tissue repair. Clin Orthop Relat Res. 2001; (391 Suppl):S26–33. [PubMed: 11603710]

6. Buckwalter JA, Mankin HJ. Articular cartilage: tissue design and chondrocyte-matrix interactions. Instr Course Lect. 1998; 47:477–86. [PubMed: 9571449]
7. Kim TK, Sharma B, Williams CG, Ruffner MA, Malik A, McFarland EG, Elisseeff JH. Experimental model for cartilage tissue engineering to regenerate the zonal organization of articular cartilage. Osteoarthritis Cartilage. 2003; 11(9):653–64. [PubMed: 12954236]
8. Ng KW, Ateshian GA, Hung CT. Zonal chondrocytes seeded in a layered agarose hydrogel create engineered cartilage with depth-dependent cellular and mechanical inhomogeneity. Tissue Eng Part A. 2009; 15(9):2315–24. [PubMed: 19231936]
9. Klein TJ, Malda J, Sah RL, Hutmacher DW. Tissue engineering of articular cartilage with biomimetic zones. Tissue Eng Part B Rev. 2009; 15(2):143–57. [PubMed: 19203206]
10. Klein TJ, Schumacher BL, Schmidt TA, Li KW, Voegtline MS, Masuda K, Thonar EJ, Sah RL. Tissue engineering of stratified articular cartilage from chondrocyte subpopulations. Osteoarthritis Cartilage. 2003; 11(8):595–602. [PubMed: 12880582]
11. Cheng C, Conte E, Pleshko-Camacho N, Hidaka C. Differences in matrix accumulation and hypertrophy in superficial and deep zone chondrocytes are controlled by bone morphogenetic protein. Matrix Biol. 2007; 26(7):541–53. [PubMed: 17618099]
12. Sharma B, Williams CG, Kim TK, Sun D, Malik A, Khan M, Leong K, Elisseeff JH. Designing zonal organization into tissue-engineered cartilage. Tissue Eng. 2007; 13(2):405–14. [PubMed: 17504064]
13. Sheehy EJ, Vinardell T, Buckley CT, Kelly DJ. Engineering osteochondral constructs through spatial regulation of endochondral ossification. Acta Biomater. 2013; 9(3):5484–92. [PubMed: 23159563]
14. Levingstone TJ, Ramesh A, Brady RT, Brama PA, Kearney C, Gleeson JP, O'Brien FJ. Cell-free multi-layered collagen-based scaffolds demonstrate layer specific regeneration of functional osteochondral tissue in caprine joints. Biomaterials. 2016; 87:69–81. [PubMed: 26901430]
15. Levingstone TJ, Thompson E, Matsiko A, Schepens A, Gleeson JP, O'Brien FJ. Multi-layered collagen-based scaffolds for osteochondral defect repair in rabbits. Acta Biomater. 2016; 32:149–60. [PubMed: 26724503]
16. Yoo JU, Barthel TS, Nishimura K, Solchaga L, Caplan AI, Goldberg VM, Johnstone B. The chondrogenic potential of human bone-marrow-derived mesenchymal progenitor cells. J Bone Joint Surg Am. 1998; 80(12):1745–57. [PubMed: 9875932]
17. Pittenger MF, Mackay AM, Beck SC, Jaiswal RK, Douglas R, Mosca JD, Moorman MA, Simonetti DW, Craig S, Marshak DR. Multilineage potential of adult human mesenchymal stem cells. Science. 1999; 284(5411):143–7. [PubMed: 10102814]
18. Kim, M., Burdick, JA., Mauck, RL. Influence of chondrocyte zone on co-culture with mesenchymal stem cells in HA hydrogels for cartilage tissue engineering. Proceedings of the ASME 2012 Summer Bioengineering Conference; June 20–23; Farjardo, Puerto Rico, USA. 2012.
19. Nazempour A, Van Wie BJ. Chondrocytes, Mesenchymal Stem Cells, and Their Combination in Articular Cartilage Regenerative Medicine. Ann Biomed Eng. 2016; 44(5):1325–54. [PubMed: 26987846]
20. O'Connell GD, Lima EG, Bian L, Chahine NO, Albro MB, Cook JL, Ateshian GA, Hung CT. Toward engineering a biological joint replacement. J Knee Surg. 2012; 25(3):187–96. [PubMed: 23057137]
21. Cigan AD, Nims RJ, Vunjak-Novakovic G, Hung CT, Ateshian GA. Optimizing nutrient channel spacing and revisiting TGF-beta in large engineered cartilage constructs. J Biomech. 2016; 49(10): 2089–94. [PubMed: 27255605]
22. Cigan AD, Durney KM, Nims RJ, Vunjak-Novakovic G, Hung CT, Ateshian GA. Nutrient Channels Aid the Growth of Articular Surface-Sized Engineered Cartilage Constructs. Tissue Eng Part A. 2016; 22(17–18):1063–74. [PubMed: 27481330]
23. Nims RJ, Cigan AD, Albro MB, Vunjak-Novakovic G, Hung CT, Ateshian GA. Matrix Production in Large Engineered Cartilage Constructs Is Enhanced by Nutrient Channels and Excess Media Supply. Tissue Eng Part C Methods. 2015; 21(7):747–57. [PubMed: 25526931]

24. Bian L, Angione SL, Ng KW, Lima EG, Williams DY, Mao DQ, Ateshian GA, Hung CT. Influence of decreasing nutrient path length on the development of engineered cartilage. Osteoarthritis Cartilage. 2009; 17(5):677–85. [PubMed: 19022685]
25. Luo L, O'Reilly AR, Thorpe SD, Buckley CT, Kelly DJ. Engineering zonal cartilaginous tissue by modulating oxygen levels and mechanical cues through the depth of infrapatellar fat pad stem cell laden hydrogels. J Tissue Eng Regen Med. 2016
26. Cigan AD, Nims RJ, Albro MB, Vunjak-Novakovic G, Hung CT, Ateshian GA. Nutrient channels and stirring enhanced the composition and stiffness of large cartilage constructs. J Biomech. 2014; 47(16):3847–54. [PubMed: 25458579]
27. Saxena V, Kim M, Keah NM, Neuwirth AL, Stoeckl BD, Bickard K, Restle DJ, Salowe R, Wang MY, Steinberg DR, Mauck RL. Anatomic Mesenchymal Stem Cell-Based Engineered Cartilage Constructs for Biologic Total Joint Replacement. Tissue Eng Part A. 2016; 22(3–4):386–95. [PubMed: 26871863]
28. Rowland CR, Colucci LA, Guilak F. Fabrication of anatomically-shaped cartilage constructs using decellularized cartilage-derived matrix scaffolds. Biomaterials. 2016; 91:57–72. [PubMed: 26999455]
29. Vaughan BL Jr, Galie PA, Stegemann JP, Grotberg JB. A poroelastic model describing nutrient transport and cell stresses within a cyclically strained collagen hydrogel. Biophys J. 2013; 105(9): 2188–98. [PubMed: 24209865]
30. Kelly TA, Ng KW, Wang CC, Ateshian GA, Hung CT. Spatial and temporal development of chondrocyte-seeded agarose constructs in free-swelling and dynamically loaded cultures. J Biomech. 2006; 39(8):1489–97. [PubMed: 15990101]
31. Lima EG, Durney KM, Sirsi SR, Nover AB, Ateshian GA, Borden MA, Hung CT. Microbubbles as biocompatible porogens for hydrogel scaffolds. Acta Biomater. 2012; 8(12):4334–41. [PubMed: 22868194]
32. Buckley CT, Thorpe SD, Kelly DJ. Engineering of large cartilaginous tissues through the use of microchanneled hydrogels and rotational culture. Tissue Eng Part A. 2009; 15(11):3213–20. [PubMed: 19374490]
33. Tharakan JP, Chau PC. Modeling and analysis of radial flow mammalian cell culture. Biotechnol Bioeng. 1987; 29(6):657–71. [PubMed: 18576500]
34. Chen CT, Fishbein KW, Torzilli PA, Hilger A, Spencer RG, Horton WE Jr. Matrix fixed-charge density as determined by magnetic resonance microscopy of bioreactor-derived hyaline cartilage correlates with biochemical and biomechanical properties. Arthritis Rheum. 2003; 48(4):1047–56. [PubMed: 12687548]
35. Kim M, Bi X, Horton WE, Spencer RG, Camacho NP. Fourier transform infrared imaging spectroscopic analysis of tissue engineered cartilage: histologic and biochemical correlations. J Biomed Opt. 2005; 10(3):031105. [PubMed: 16229630]
36. Potter K, Butler JJ, Adams C, Fishbein KW, McFarland EW, Horton WE, Spencer RG. Cartilage formation in a hollow fiber bioreactor studied by proton magnetic resonance microscopy. Matrix Biol. 1998; 17(7):513–23. [PubMed: 9881603]
37. Huang AH, Stein A, Mauck RL. Evaluation of the complex transcriptional topography of mesenchymal stem cell chondrogenesis for cartilage tissue engineering. Tissue Eng Part A. 2010; 16(9):2699–708. [PubMed: 20367254]
38. Huang AH, Yeger-McKeever M, Stein A, Mauck RL. Tensile properties of engineered cartilage formed from chondrocyte- and MSC-laden hydrogels. Osteoarthritis Cartilage. 2008; 16(9):1074–82. [PubMed: 18353693]
39. Mauck RL, Wang CC, Oswald ES, Ateshian GA, Hung CT. The role of cell seeding density and nutrient supply for articular cartilage tissue engineering with deformational loading. Osteoarthritis Cartilage. 2003; 11(12):879–90. [PubMed: 14629964]
40. Burdick JA, Chung C, Jia X, Randolph MA, Langer R. Controlled degradation and mechanical behavior of photopolymerized hyaluronic acid networks. Biomacromolecules. 2005; 6(1):386–91. [PubMed: 15638543]

41. Mackay AM, Beck SC, Murphy JM, Barry FP, Chichester CO, Pittenger MF. Chondrogenic differentiation of cultured human mesenchymal stem cells from marrow. Tissue Eng. 1998; 4(4): 415–28. [PubMed: 9916173]
42. Mauck RL, Yuan X, Tuan RS. Chondrogenic differentiation and functional maturation of bovine mesenchymal stem cells in long-term agarose culture. Osteoarthritis Cartilage. 2006; 14(2):179–89. [PubMed: 16257243]
43. Schinagl RM, Gurskis D, Chen AC, Sah RL. Depth-dependent confined compression modulus of full-thickness bovine articular cartilage. J Orthop Res. 1997; 15(4):499–506. [PubMed: 9379258]
44. Farrell MJ, Comeau ES, Mauck RL. Mesenchymal stem cells produce functional cartilage matrix in three-dimensional culture in regions of optimal nutrient supply. Eur Cell Mater. 2012; 23:425–40. [PubMed: 22684531]
45. Farndale RW, Buttle DJ, Barrett AJ. Improved quantitation and discrimination of sulphated glycosaminoglycans by use of dimethylmethylene blue. Biochim Biophys Acta. 1986; 883(2):173–7. [PubMed: 3091074]
46. Neuman RE, Logan MA. The determination of hydroxyproline. J Biol Chem. 1950; 184(1):299–306. [PubMed: 15421999]
47. Darling EM, Athanasiou KA. Rapid phenotypic changes in passaged articular chondrocyte subpopulations. J Orthop Res. 2005; 23(2):425–32. [PubMed: 15734258]
48. Hong E, Reddi AH. Dedifferentiation and redifferentiation of articular chondrocytes from surface and middle zones: changes in microRNAs-221/-222, -140, and-143/145 expression. Tissue Eng Part A. 2013; 19(7–8):1015–22. [PubMed: 23190381]
49. Chen X, Liang H, Zhang J, Zen K, Zhang CY. Secreted microRNAs: a new form of intercellular communication. Trends Cell Biol. 2012; 22(3):125–32. [PubMed: 22260888]
50. Farrell MJ, Fisher MB, Huang AH, Shin JI, Farrell KM, Mauck RL. Functional properties of bone marrow-derived MSC-based engineered cartilage are unstable with very long-term in vitro culture. J Biomech. 2014; 47(9):2173–82. [PubMed: 24239005]
51. Hung CT, Lima EG, Mauck RL, Takai E, LeRoux MA, Lu HH, Stark RG, Guo XE, Ateshian GA. Anatomically shaped osteochondral constructs for articular cartilage repair. J Biomech. 2003; 36(12):1853–64. [PubMed: 14614939]

Statement of Significance

Articular cartilage is a highly organized tissue driven by zonal heterogeneity of cells, extracellular matrix proteins and fibril orientations, raising depth-dependent mechanical properties. Therefore, the recapitulation of the functional properties of native cartilage in a tissue engineered construct requires such a biomimetic design of the morphological organization, and this has remained a challenge in cartilage tissue engineering. This study demonstrates that a layer-by-layer fabrication scheme, including co-cultures of zone-specific articular CHs and MSCs, can reproduce the depth-dependent characteristics and mechanical properties of native cartilage while minimizing the need for large numbers of chondrocytes. In addition, an introduction of a porous hollow fiber (combined with a cotton thread) enhances nutrient transport and depth-dependent properties of the tri-layered construct. Such a tri-layered construct may provide critical advantages for focal cartilage repair. These constructs hold promise for restoring native tissue structure and function, and may be beneficial in terms of zone-to-zone integration with adjacent host tissue and providing more appropriate strain transfer after implantation.

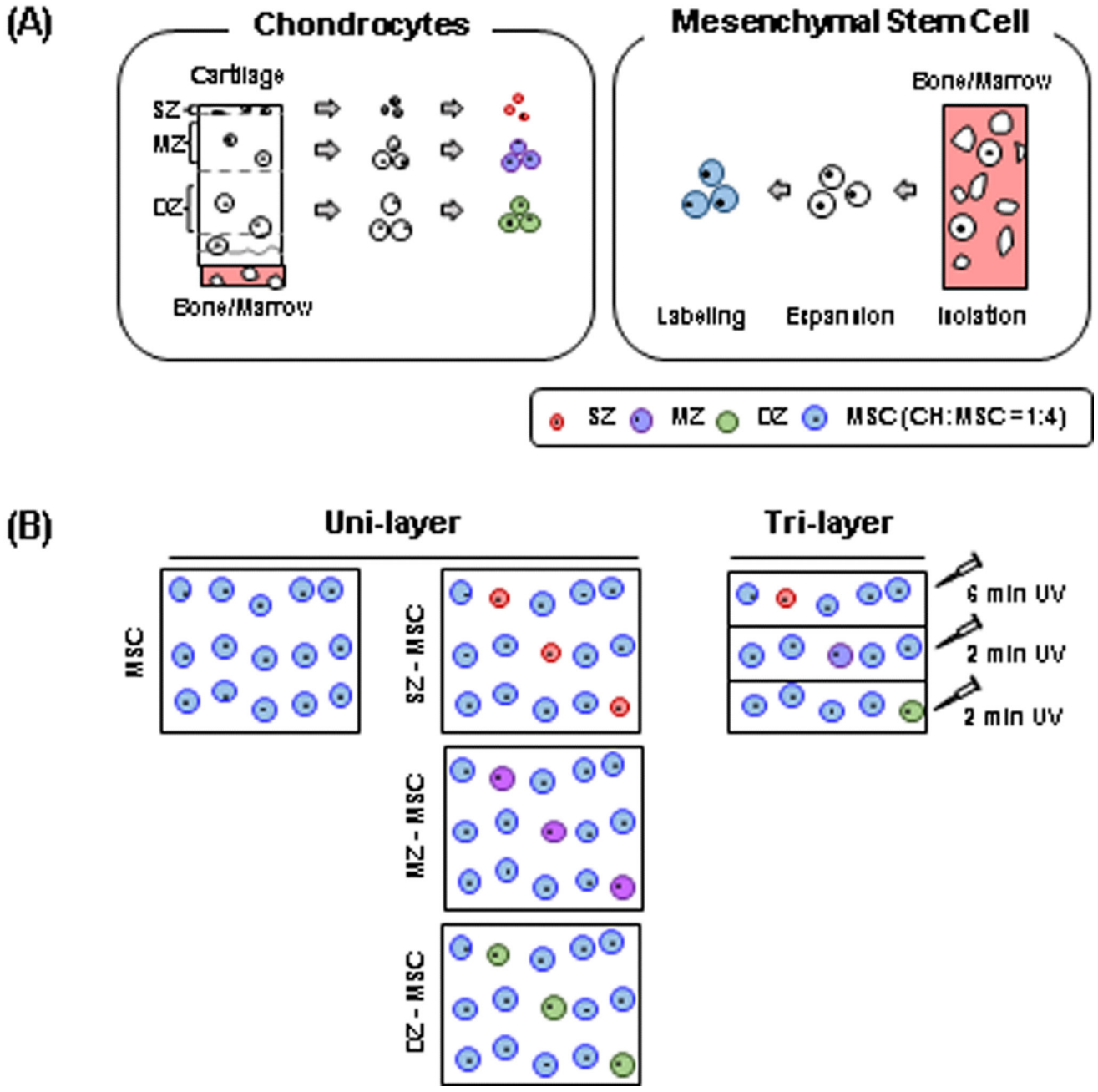

Figure. 1. A Schematic of a tri-layered construct fabrication with zonal CH/MSC co-culture

(A) Zonal chondrocytes (SZ, MZ and DZ; left) and MSCs (right) were isolated from articular cartilage and bone marrow, respectively. Isolated cells were expanded in culture separately and labeled with CellTracker (SZ: red, MZ: purple, DZ: green and MSC: blue) to trace the distribution of cell subpopulations during long-term culture. (B) Fabrication procedure for single- and tri-layered constructs.

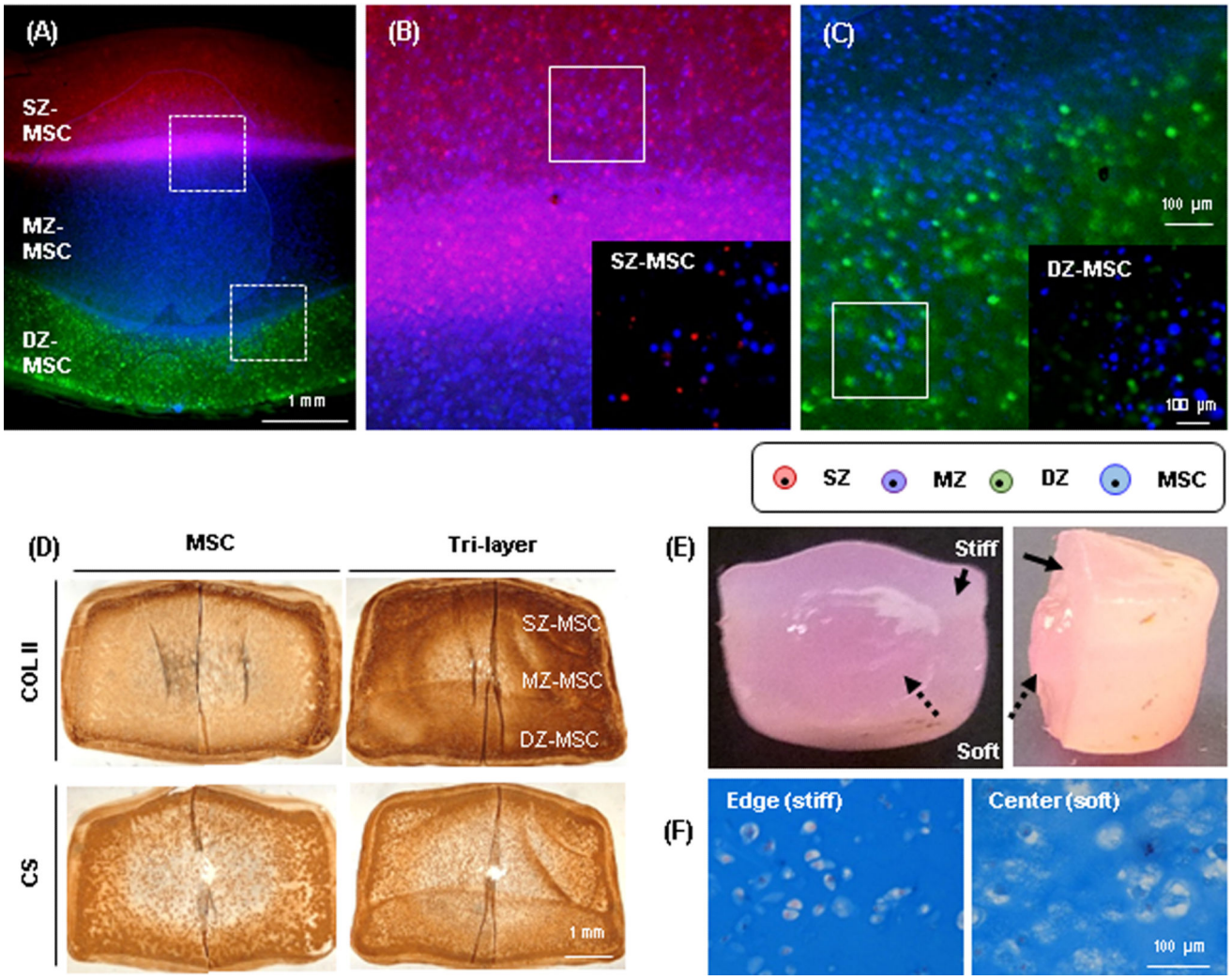

Figure. 2. Development and maturation of a tri-layered construct

(A) A cross-sectional view of a tri-layered construct showing distinct zonal sub-layers visualized by CellTracker at 16 weeks (SZ CH: red, MZ: purple, DZ: green and MSC: blue; Top layer: SZ-MSC, Middle: MZ-MSC and Bottom: DZ-MSC; scale bar = 1 mm). (B–C) Zoomed views of the dashed boxes showing cells and interface of (B) top-middle and (C) middle-bottom layer (scale bar = 100 μm). Co-cultures of SZ-MSC (Inset B) and DZ-MSC (Inset C) were evident in each sub-layer (20×; scale bar = 100 μm). (D) Immunohistochemistry of type II collagen (top) and chondroitin sulfate (bottom) at 8 weeks (60 million cells/mL; CH:MSC = 1:4; scale bar = 1 mm). (E) Heterogeneous matrix accumulation at 8 weeks in a tri-layered construct due to limited nutrient transport to the central region. The peripheral region (solid arrow) showed denser matrix and less swelling than the core (dashed arrow). (F) Alcian blue staining of peripheral (left) and core (right) region of the construct (20×, scale bar = 100 μm).

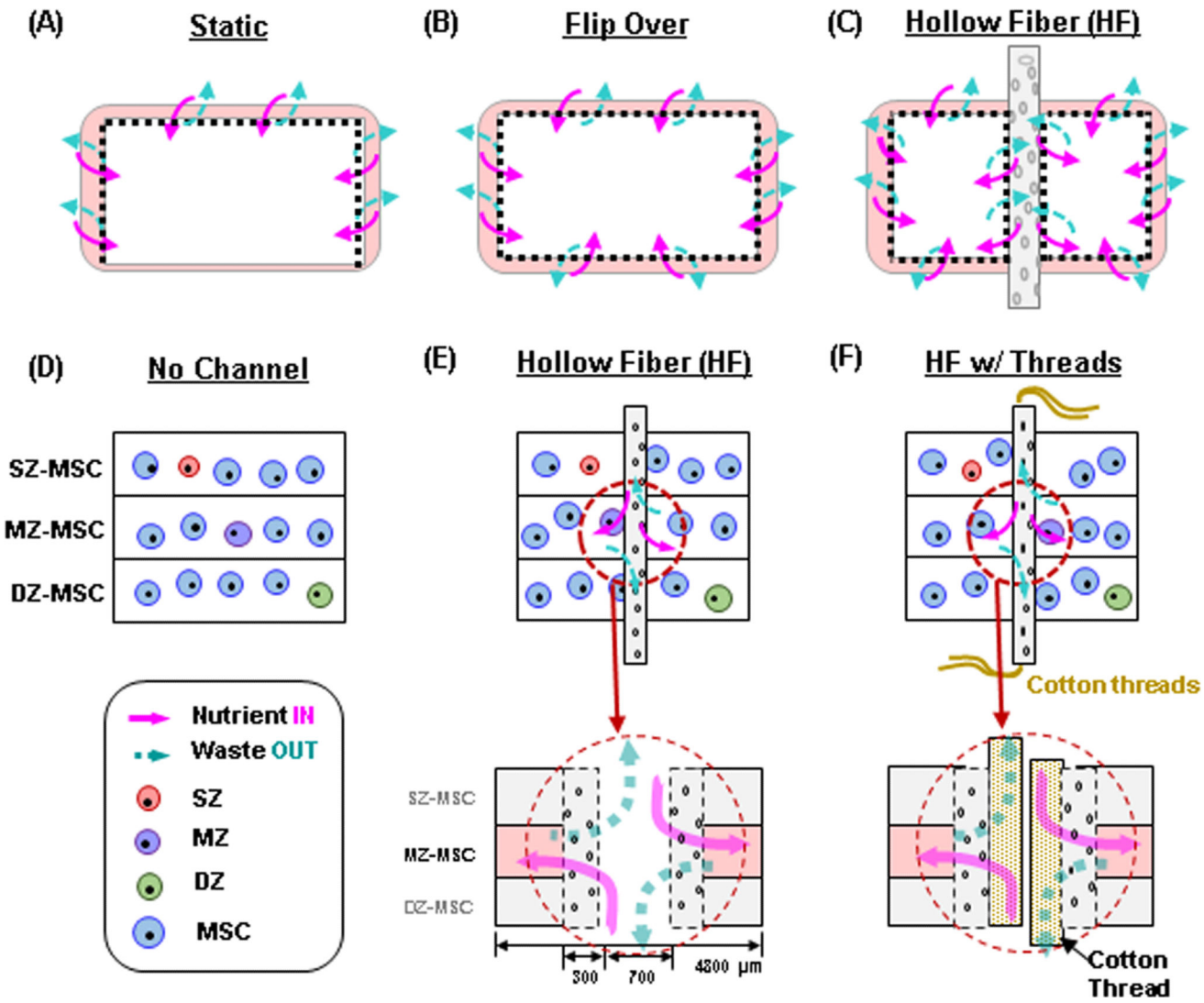

Figure. 3. Schematics showing accessible surface area for nutrient/waste transport in gel-based constructs and novel strategies to enhance transport

(A–C) Nutrient transport paths under free swelling conditions; (A) Static culture, (B) static culture where constructs are regularly flipped (Flip over), (C) static culture where transport is improved by introduction of hollow fiber (HF) channels. (D–F) HF (and HF w/cotton threads)-mediated strategies to improve nutrient transport; (D) No channel, (E) Hollow fiber (HF), (F) HF w/ cotton threads. Schematics of paths available for nutrient/waste transport by HF or HF/ cotton threads. (pink (solid) arrow = nutrient “in”, blue (dashed) arrow = waste “out”).

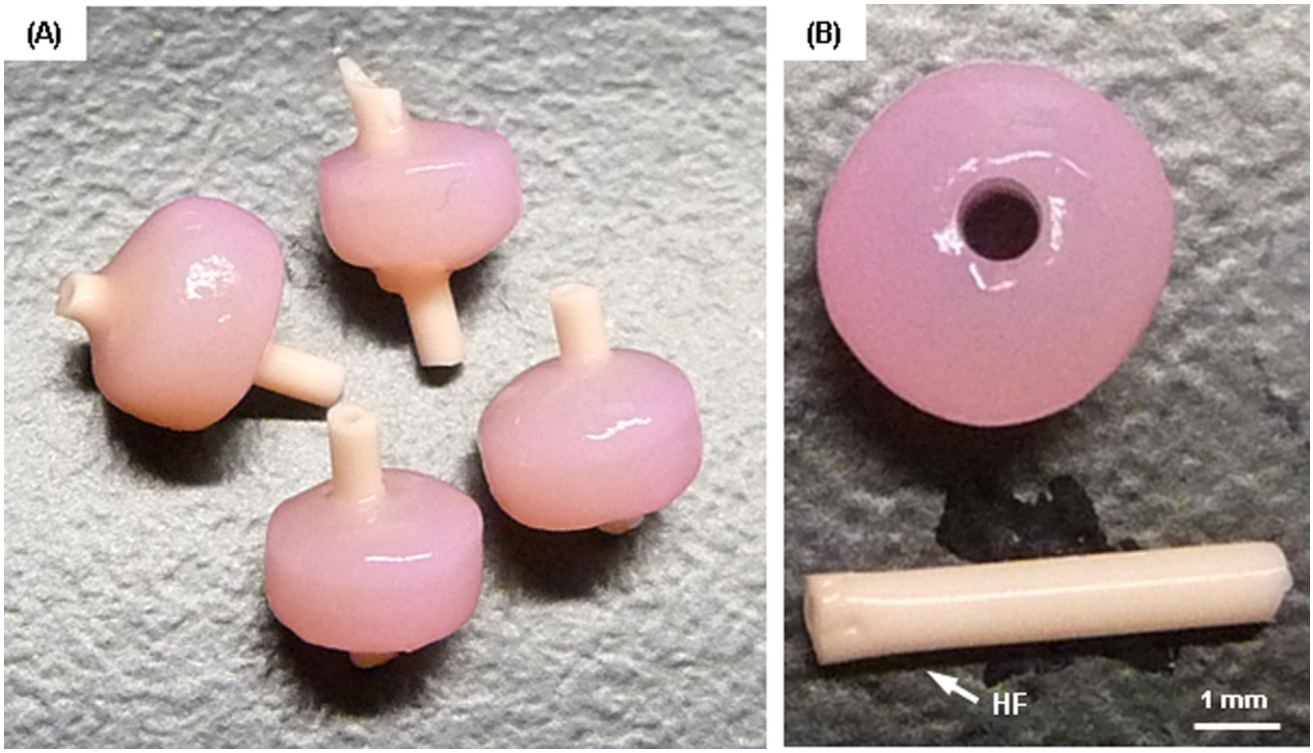

Figure. 4. Gross appearance of tri-layered constructs with hollow fiber after 8 weeks of culture

The HF channel remained open during the culture period (A), and there was little to no interaction between the HF and the surrounding hydrogel (B) (scale bar = 1 mm).

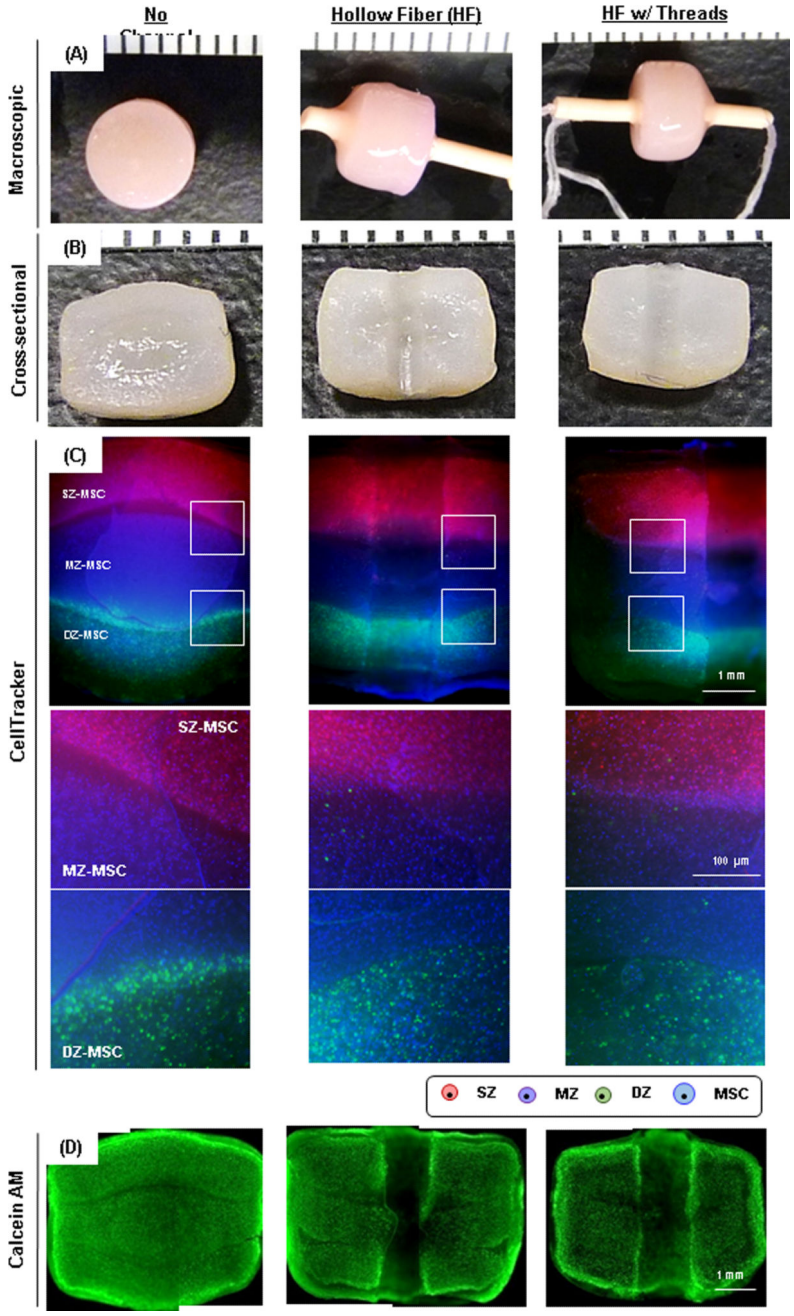

Figure. 5. Maturation of tri-layered constructs with HFs

Groups are indicated as “No Channel” (left column), “Hollow Fiber” (HF; middle) and “HF w/threads” (right), respectively. (A) Gross appearance of tri-layered constructs with 8 weeks of culture (markers = 1 mm). (B) Cross-sectional view (markers = 1 mm). (C) CellTracker-labeled zonal chondrocytes and MSCs co-cultured in a tri-layered construct (2.5×, scale bar = 1 mm). Middle and bottom images are zoomed view of the interfaces of tri-layered constructs. (D) Calcein-AM staining of constructs at 8 weeks of culture (2.5×, scale bar = 1 mm).

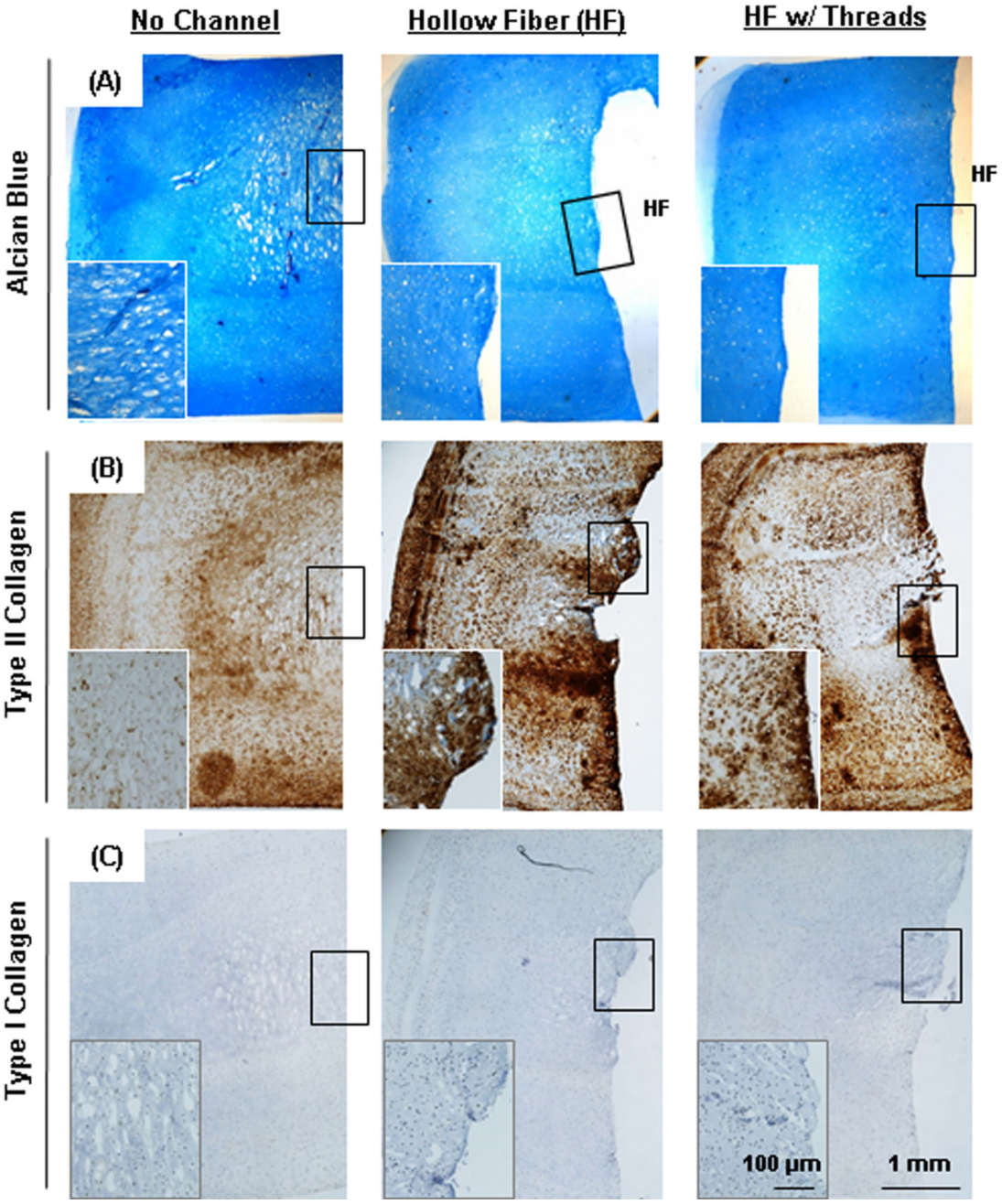

Figure. 6. Histological analysis of tri-layered construct with long-term culture

(A) Alcian blue staining and immunohistochemistry of (B) type II collagen and (C) type I collagen of constructs at 16 weeks of culture (2.5× and 10× (inset), scale bar = 1mm (inset = 100 μm)). HF indicates original position of hollow fiber.

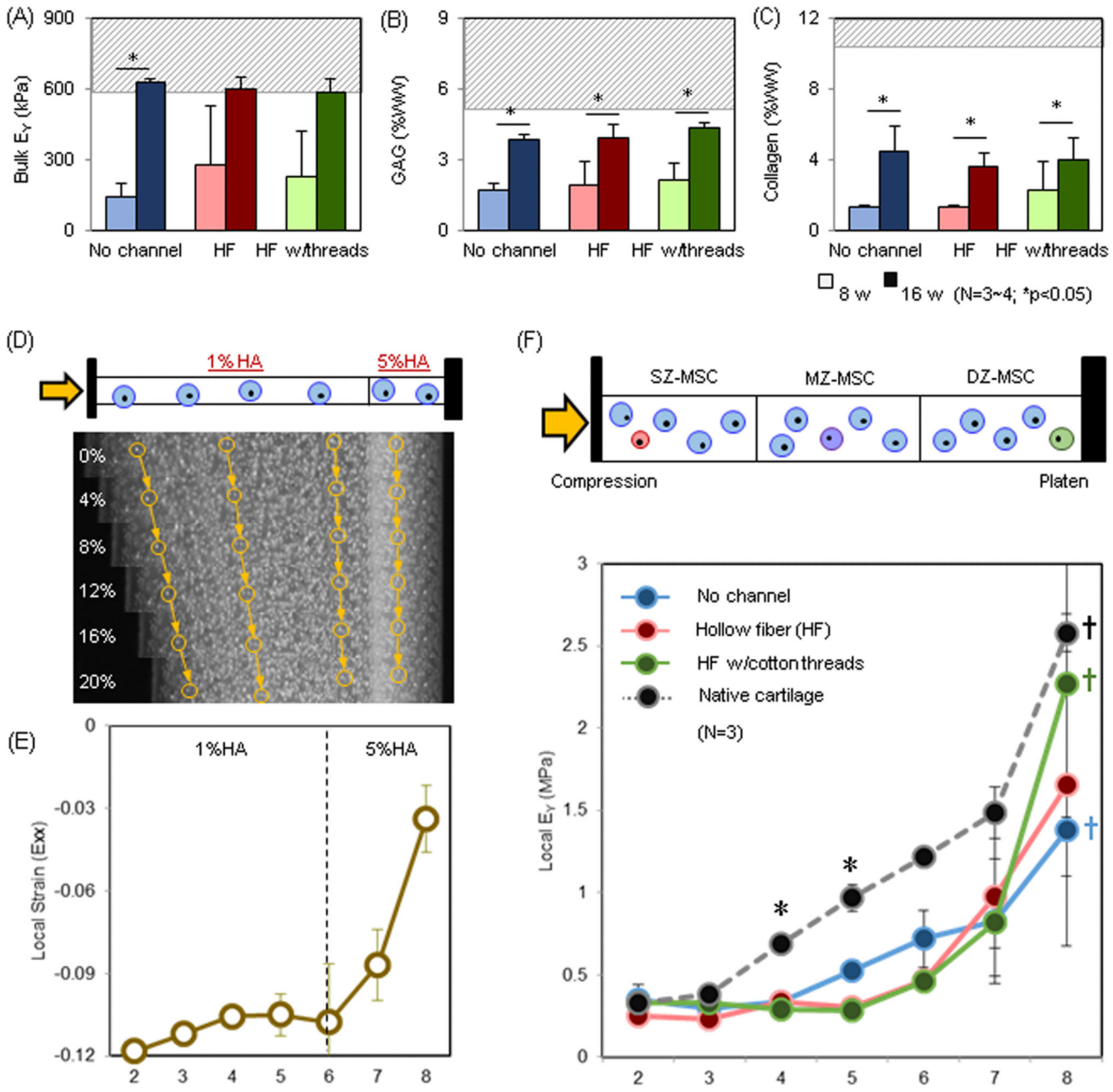

Figure. 7. Depth-dependent properties of tri-layered construct with long-term culture

(A–C) Bulk properties of tri-layered constructs: (A) E_Y (kPa; the baseline bulk E_Y of 1% MeHA is ~ 5 kPa.) (B) GAG (%WW), (C) Collagen (%WW) (Dashed gray line = native cartilage; Lighter bars = 8 weeks, Darker bars = 16 weeks). (D–E) Validation of a local compression device: (D) MSC-laden bi-layered HA constructs (1 and 5% MeHA) stained with Hoechst were subjected to compression (0% ~ 20% strain applied) and nuclei were tracked to compute local properties. Yellow arrows and circles indicate nuclei traced from reference image (0% strain) on day 0. (E) Local strain (ε_{xx}, Day 0). (F) Local E_Y (kPa) for tri-layered constructs at 16 weeks (No channel = blue, HF = red, HF w/cotton threads =

green, Native cartilage = black, n=3/group). ($p \leq 0.05$; * Native cartilage vs. Tri-layered constructs in the middle layer; † Bottom layer (#8) vs. Middle and Top layer).

Table. 1

Mechanical and biochemical properties of cell-laden HA constructs with long-term culture.

GROUP	Time (wk)	E_Y (kPa)	$\|G^*\|$ (MPa)	GAG (%WW)	Collagen (%WW)	DI (mm)
MSC	8	309 ± 89	2.1 ± 0.4	3.8 ± 0.2	2.2 ± 0.3	5.4 ± 0.1
	16	338 ± 51	2.5 ± 0.7	3.7 ± 0.4 *	7. 6 ± 1.5	5.5 ± 0.1
SZ-MSC	8	334 ± 88	1.9 ± 0.5	3.8 ± 0.5	1.9 ± 0.5	5.2 ± 0.1
	16	317 ± 47	2.0 ± 0.3	4.2 ± 1.0	3.3 ± 0.5	5.2 ± 0.1
MZ-MSC	8	377 ± 34 †	2.1 ± 0.2	4.3 ± 0.2	2.2 ± 0.2	5.4 ± 0.1
	16	481 ± 81	3.1 ± 0.4 *	4.8 ± 0.5	6.5 ± 0.9 †$	5. 6 ± 0.2
DZ-MSC	8	370 ± 11	2.1 ± 0.1	4.5 ± 0.4	2.3 ± 0.2	5.3 ± 0.1
	16	428 ± 138	2.7 ± 0.5	4.5 ± 0.5	7.3 ± 1.6 ‡^	5.7 ± 0.4
Tri-layer	8	522± 52	2.8 ± 0.3	5.0 ± 0.5	3.3 ± 1.1	5.3 ± 0.0
	16	537 ± 177 *	2.9 ± 0.9	4.4 ± 0.7	6.4 ± 2.1	5.3 ± 0.5

(Mean ± SD; N=3~4/group)

E_Y (kPa) *SM vs. Tri-layer (16w; p=0.058); †SM vs. MM (16w; p=0.058)

|G*| (MPa) *MM(8w) vs. MM(16w) (p=0.023)

Collagen (%WW) *MSC (8w) vs. MSC (16w) (p<0); $MM(8w) vs MM(16w) (p=0.001) ^DM(8w) vs. DM(16w) (p=0); †SM vs. MM (16w) (p=0.047); ‡SM vs. DM (16w) (p=0.006)